Available online at www.sciencedirect.com
ScienceDirect
Polymer 47 (2006) 7731–7739
polymer
www.elsevier.com/locate/polymer

The structure and physical properties of polypropylene and thermoplastic olefin nanocomposites containing nanosilica

Yiqun Liu, Marianna Kontopoulou*

Department of Chemical Engineering, Queen's University, Kingston, ON, Canada K7L 3N6

Received 13 June 2006; received in revised form 29 August 2006; accepted 4 September 2006
Available online 22 September 2006

Abstract

The morphology and physical properties of thermoplastic olefin blend (TPO) based nanocomposites containing nanosilica are reported. Addition of maleated PP resulted in improved filler dispersion within the PP matrix, where the filler resided exclusively. This separated morphology resulted in selective reinforcement of the PP matrix without compromising ductility, as demonstrated by mechanical property characterization. The tensile moduli, impact and flexural properties of TPO/nanosilica composites showed improvements at low loadings of nanosilica, indicating a good balance of stiffness and toughness. The addition of nanosilica into the TPOs decreased the size of the dispersed elastomer phase, which was a factor in the observed improvements of impact strength. Silane-modified nanosilica dispersed more efficiently in the polymer matrix, giving rise to improved impact properties of the TPO composites, compared to the unmodified filler.

Keywords: Polypropylene; Polyolefin elastomer; Nanocomposites

1. Introduction

Thermoplastic olefin (TPO) blends consist of polypropylene (PP) and olefinic elastomer components. Most commonly PP comprises the major phase and thus forms the matrix of the TPOs [1–4]. The dispersed elastomer phase serves to improve the toughness and low-temperature impact resistance of PP. However, presence of the elastomeric component inevitably has a detrimental effect on the stiffness of the material [5].

Inorganic fillers are commonly added in TPO formulations to increase their stiffness, improve their dimensional stability, and lower the cost of the compounds. Various PP/elastomer/filler ternary systems containing fillers such as $CaCO_3$, talc and silica have been investigated in the past [6–11]. When fillers are added in PP/elastomer blends, and depending on the location of the filler, three types of microstructures may form: ''separate'' dispersion structure, where the filler resides in the matrix, encapsulation/core–shell structure, where the filler partitions preferentially in the dispersed phase, and mixtures of the former two. A separated microstructure, wherein the filler partitions favourably in the PP matrix, without affecting the elastomer phase, is desirable for optimum reinforcement of TPO blends [6–8].

Recent reports have highlighted the effects of addition of organoclay-type nanofillers into TPOs [12–17]. Although introduction of clay into the TPOs improves their flexural and tensile moduli, this is generally counteracted by decreases in elongation [17]. Lee and Goettler [14] used different addition sequences during compounding to control the localization of the clay, thus significantly affecting the mechanical properties of the compounds. Lee et al. [12] studied systematically the morphology and mechanical properties of a PP/ethylene–octene elastomer/clay system, and found that the reduction in size of elastomer particles taking place in the presence of clay particles affected favourably the impact properties of the material.

Besides organoclay, other nanofillers such as nanosilica can also serve as reinforcing agents. Silica has been widely used

* Corresponding author. Tel.: +1 613 533 3079; fax: +1 613 533 6637.
E-mail address: marianna.kontopoulou@chee.queensu.ca (M. Kontopoulou).

0032-3861/$ - see front matter © 2006 Elsevier Ltd. All rights reserved.
doi:10.1016/j.polymer.2006.09.014

as reinforcing filler in the rubber industry. Several research studies pertaining to its application in PP reinforcement have been published in recent years [18–21]. Due to the non-polar nature of PP and the large surface area of polar nanosilica particles, it is challenging to achieve good dispersion of nanosilica into a PP matrix. Efforts have centered on improving the dispersion of nanosilica in PP by modifying the filler through irradiation grafting [18,19], using surface treated nanosilica [21], or adding maleated PP as a compatibilizer [20]. These studies revealed that reinforcement can be achieved at relatively low filler loadings, between 2.5 and 5 wt%.

In our previous work [22,23], we have reported that when added to polyolefin blends, high energy fillers such as organoclay and nanosilica migrate into the maleated phase. In this work we aim at taking advantage of this trait to preferentially localize the filler inside the PP matrix, thus selectively reinforcing it, without affecting the toughening ability of the dispersed ethylene–octene copolymer elastomer phase. The structure and properties of the resulting TPO nanocomposites are presented. The properties of the PP matrix/nanosilica filled composites were also studied to provide a suitable reference.

2. Experimental

2.1. Materials

PP homopolymer, Escorene® 1042, MFR 1.9 g/10 min at 230 °C, was supplied by ExxonMobil Chemical. An ethylene–octene copolymer polyolefin elastomer (POE, Engage® 8100, MFR 1.0 g/10 min at 190 °C, from DuPont Dow Elastomers) was used as an impact modifier. Maleated PP (PP-*g*-MAn), Fusabond® PMD 511D, MFR 24 g/10 min at 190 °C, containing 0.25–0.5% maleic anhydride was supplied by E.I. DuPont Canada. Nanosilica (SiO_2), Aerosil® 200, with a measured specific surface of 200 m^2/g, and modified nanosilica ($mSiO_2$), treated with trimethoxyoctylsilane, Aerosil® R805, having a specific surface of 150 m^2/g, were supplied by Degussa Corp. Irganox 225 antioxidant was obtained from Ciba–Geigy.

2.2. Compounding procedure

All blends and composites were prepared in a Haake PolyLab torque rheometer equipped with a Rheomix 610p mixing chamber and roller rotors. The components of 40 g were loaded to the mixing chamber simultaneously and compounded at 200 °C for 4 min, with a rotor speed of 60 rpm. Antioxidant of 0.08 g (0.2 wt%) was added to all formulations. PP composites containing 0–7 wt% nanosilica and PP/POE blends containing 10–30 wt% POE and 0–7 wt% nanosilica were prepared. All compositions are listed in detail in Tables 1 and 2. The component ratio and filler loadings are reported on a weight basis.

2.3. Mechanical properties

Tensile properties were measured using an Instron 3369 universal tester, at crosshead speeds of 10 or 50 mm/min for the PPs and TPOs, respectively. Dumbbell-shaped specimens were cut with a Type V die according to ASTM D638 from 1.5 mm thick sheets, which were prepared by compression molding of the compounded samples at approximately 200 °C using a Carver press.

Notched Izod impact tests were carried out on an Instron BLI impact tester at room temperature according to ASTM D256. Specimens of dimensions $64 \times 12.7 \times 3.2$ mm were prepared by compression molding at 200 °C. At least 5 samples were tested for each sample and the average values were reported.

Flexural tests were performed according to ASTM D790, procedure B, at a speed of 13.65 mm/min. Rectangular bars of dimensions $127 \times 12.7 \times 3.2$ mm were produced by compression molding at 200 °C.

2.4. Microscopy and image analysis

The state of dispersion of the filler in the polymer blends was assessed by TEM imaging, using an FEI Tecnai 20 instrument. Ultra-thin sections were cryomicrotomed using a Leica ultra microtome and stained in RuO_4 vapour to enhance the phase contrast between the PP and elastomer phases.

For SEM observations compression molded samples were cryomicrotomed on a RMC Power Tome X microtome using a glass knife at −100 °C to obtain flat surfaces, and then etched in toluene at 70 °C for 2 h to remove the dispersed elastomer phase. The etched surfaces were observed on a JEOL JSM-840 scanning electron microscope. The SEM images were analyzed by using the Sigma Scan Pro image analysis software to estimate the average diameters of the dispersed elastomer phase.

2.5. Thermal properties

The melting and crystallization temperatures, as well as heat of fusion and crystallization of the samples were measured on a TA Q100 differential scanning calorimeter (DSC).

Table 1
Tensile properties of PP/PP-*g*-MAn blends and their composites (tensile testing speed 10 mm/min)

Composition		Young's modulus (MPa)	Yield stress (MPa)	Elongation at break (%)
Ratio of PP/PP-*g*-MAn	SiO_2 content (wt%)			
100/0	0	367 ± 21	30.6 ± 1.6	1660 ± 120
95/5	0	372 ± 16	30.9 ± 1.1	1680 ± 120
90/10	0	358 ± 32	30.0 ± 1.0	1680 ± 140
80/20	0	351 ± 16	29.6 ± 0.9	1690 ± 200
100/0	5	393 ± 15	31.8 ± 0.5	1180 ± 270
95/5	5	383 ± 19	30.8 ± 0.9	1490 ± 100
90/10	5	403 ± 21	32.6 ± 1.1	1270 ± 200
80/20	5	387 ± 24	30.6 ± 1.2	1430 ± 40
90/10	5 ($mSiO_2$)	384 ± 16	30.1 ± 0.4	1550 ± 60

Table 2
Tensile and crystallization properties of TPO blends and composites (tensile testing speed 50 mm/min)

Composition		Young's modulus (MPa)	Tensile stress (MPa)[b]	Elongation at break (%)	Crystallization temperature (°C)	Heat of crystallization[c] (J/g)
PP matrix[a]/POE	SiO_2 (wt%)					
100/0	0	398 ± 25	33.7 ± 1.5 (33.7 ± 1.5)	930 ± 220	113.3	100
90/10	0	324 ± 8	26.6 ± 0.6 (33.7 ± 6.1)	1400 ± 280	112.3	96
90/10	5	337 ± 8	27.9 ± 0.6 (28.2 ± 0.6)	1030 ± 300	114.3	94
80/20	0	265 ± 15	22.8 ± 0.9 (40.1 ± 4.2)	1750 ± 130	111.9	95
80/20	2	278 ± 11	22.7 ± 0.3 (34.7 ± 10.8)	1360 ± 600	113.0	97
80/20	5	304 ± 17	23.6 ± 1.0 (34.5 ± 4.7)	1440 ± 280	114.8	101
80/20	7	285 ± 8	22.5 ± 1.2 (25.8 ± 4.4)	1380 ± 290	115.1	100
80/20	5 (mSiO2)	313 ± 7	24.3 ± 0.8 (34.3 ± 6.3)	1470 ± 420	112.9	96
70/30	0	228 ± 8	18.8 ± 0.8 (37.5 ± 4.8)	1660 ± 180	110.1	97
70/30	5	233 ± 12	19.4 ± 0.4 (33.3 ± 5.6)	1490 ± 230	115.6	94

[a] PP matrix composition: PP/PP-*g*-MAn 90/10.
[b] Tensile stress at yield. Values in parenthesis represent tensile stress at break.
[c] Based on PP component.

The samples were first heated to 230 °C for 2 min to eliminate their thermal history and subsequently cooled to 25 °C at a rate of 10 °C/min. The second endotherm was recorded by heating at 10 °C/min.

2.6. Rheology

Rheological characterization was carried out on a Reologica ViscoTech oscillatory rheometer using 20 mm parallel plate fixtures, with a gap of 1 mm at 200 °C, under a nitrogen blanket. The rheometer was operated in the dynamic oscillatory mode in the linear viscoelasticity region. The elastic modulus (G'), loss modulus (G'') and complex viscosity (η^*) were measured as a function of angular frequency (ω).

2.7. X-ray diffraction

Wide angle X-ray diffraction (XRD) was used to evaluate the PP crystal structure. Films with approximately 400 nm thick were prepared by compression molding and scanned in a 2θ range from 1° to 50° at a rate of 1°/min using a Scintag Model X1 powder X-ray diffractometer (Cu Kα radiation, $\lambda = 1.5406$ Å, generator voltage = 45 kV, current = 40 mA). Measurements were recorded at every 0.03° interval.

3. Results and discussion

3.1. Structure and properties of PP/SiO_2 composites

The presence of large SiO_2 agglomerates within the PP matrix, shown in the TEM micrographs (Fig. 1a), provides evidence of the poor interaction between the polar filler and the non-polar polyolefin matrix. Incorporation of 10 wt% PP-*g*-MAn clearly enhanced the dispersion of the filler (Fig. 1b). In spite of this improvement, SiO_2 still existed in the form of small aggregates, comprising several primary particles, as shown by TEM images taken at higher magnification (Fig. 1c). The silane-treated $mSiO_2$ was dispersed more effectively compared to the unmodified SiO_2 (Fig. 1d), suggesting that the surface modification increased the affinity of the filler to the PP/PP-*g*-MAn matrix.

Given that the addition of PP-*g*-MAn can affect the mechanical properties of the matrix, we investigated the effect of PP-*g*-MAn content on the tensile properties of the PP matrix, in order to determine a PP-*g*-MAn/PP ratio that would not compromise significantly its properties. Within experimental error, reductions in Young's modulus, yield stress and elongation were minor, up to a ratio of PP/PP-*g*-MAn 80/20 (Table 1).

All SiO_2 filled PP/PP-*g*-MAn composites exhibited improved moduli and small reductions in elongation at break with respect to their base blend (Table 1). Composites containing PP-*g*-MAn showed more substantial improvements in modulus and better elongation at break than the samples containing only PP, due to the improved dispersion of SiO_2 in the presence of PP-*g*-MAn. Samples containing $mSiO_2$ displayed higher elongation at break than their counterparts containing unmodified SiO_2, which once again is attributed to the significantly better dispersion of $mSiO_2$ (Fig. 1d).

The PP-*g*-MAn/PP matrix was very brittle, having an impact strength of 28.9 ± 1.6 J/m. Addition of SiO_2 did not affect negatively the impact properties of the polymer, but actually resulted in a slight increase; the values of impact strength upon addition of 5 wt% SiO_2 and $mSiO_2$ were 34.9 ± 3 J/m and 30.3 ± 3 J/m, respectively. These results are consistent with the findings of Bikiaris et al. [20,21] and Rong et al. [18], who reported that the impact strength and fracture energy of PP improved upon addition of low amounts of nanosilica and ascribed this to good interfacial interaction between polymer and nanofiller.

Due to the low aspect ratio of nanosilica fillers compared to their organoclay counterparts, addition of SiO_2 resulted in only marginal increases in the complex viscosity and storage modulus of the composites (Fig. 2a and b). Addition of $mSiO_2$ had the least effect, even though the filler was better dispersed, apparently due to the surface treatment of the filler. Surface treatment can cause a reduction in viscosity, as it acts to wet and disperse the fillers, or to lubricate the filler surface so that there is slippage between polymer and filler [24].

Given that high PP-*g*-MAn contents are undesirable from a practical standpoint and that the samples containing 10 wt% PP-*g*-MAn exhibited good SiO_2 dispersion and mechanical

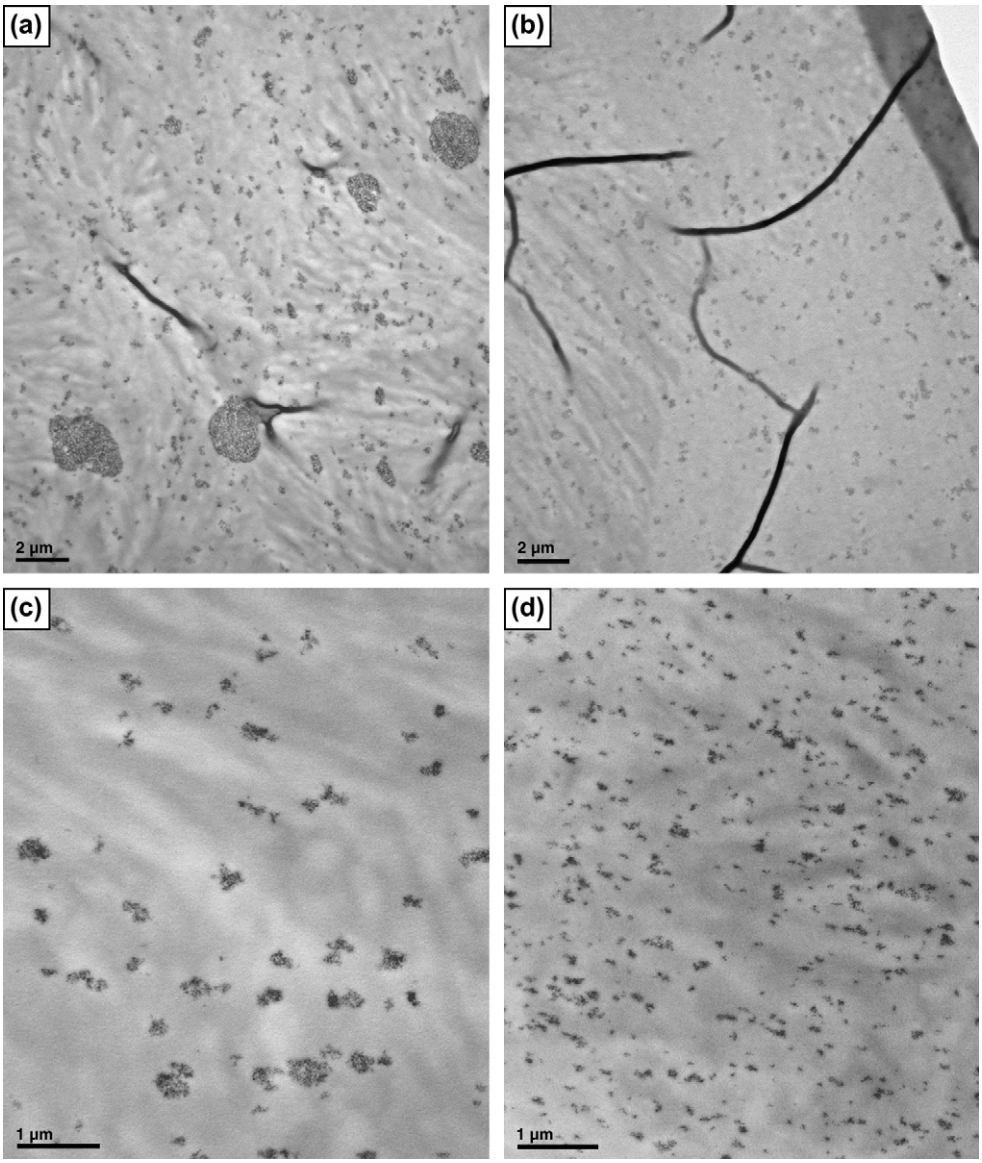

Fig. 1. TEM micrographs of PP/nanosilica composites: (a) PP/5 wt% SiO_2; (b), (c) (PP/PP-*g*-MAn 90/10)/5 wt% SiO_2; (d) (PP/PP-*g*-MAn 90/10)/5 wt% $mSiO_2$. Scale bars represent 2 μm in (a), (b), and 1 μm in (c), (d).

properties, a ratio of PP/PP-*g*-MAn 90/10 was chosen for the subsequent studies on the TPO system.

3.2. TPO/nanosilica composites

3.2.1. Structure and morphology

As mentioned in Section 1, a separated microstructure, where the filler partitions favourably in the PP matrix without affecting the elastomer phase, is desirable for optimum reinforcement in TPOs. TEM micrographs of TPO/nanosilica composites (Fig. 3) show that nanosilica localized exclusively in the PP/PP-*g*-MAn matrix phase and formed the desired separated microstructure (Fig. 3a). In agreement with the results presented above on the PP-based composites, the filler dispersion within the PP matrix was significantly improved when the silane-modified silica, $mSiO_2$, was used (Fig. 3b).

Consistently with previous reports on TPOs [12,16], as well as on a multitude of other immiscible blends [25,26], in our blends the size of the dispersed phase was reduced in the presence of the nanofiller and the particle size distribution became narrower, as shown in the SEM images presented in Fig. 4 and the results obtained from image analysis (Fig. 5).

Although numerous explanations exist on the effect of platelet-like fillers, such as organoclays, on the morphology of immiscible blends [25,26], the effect of nanosilica is less evident, given that it essentially consists of spherical primary particles. As demonstrated in Fig. 2, the rheological properties of the PP/PP-*g*-MAn matrix were not significantly altered in the presence of SiO_2, and therefore the viscosity ratio between the matrix and the POE dispersed phase remained essentially the same; therefore the decrease in the size of the dispersed phase could not have resulted from a change

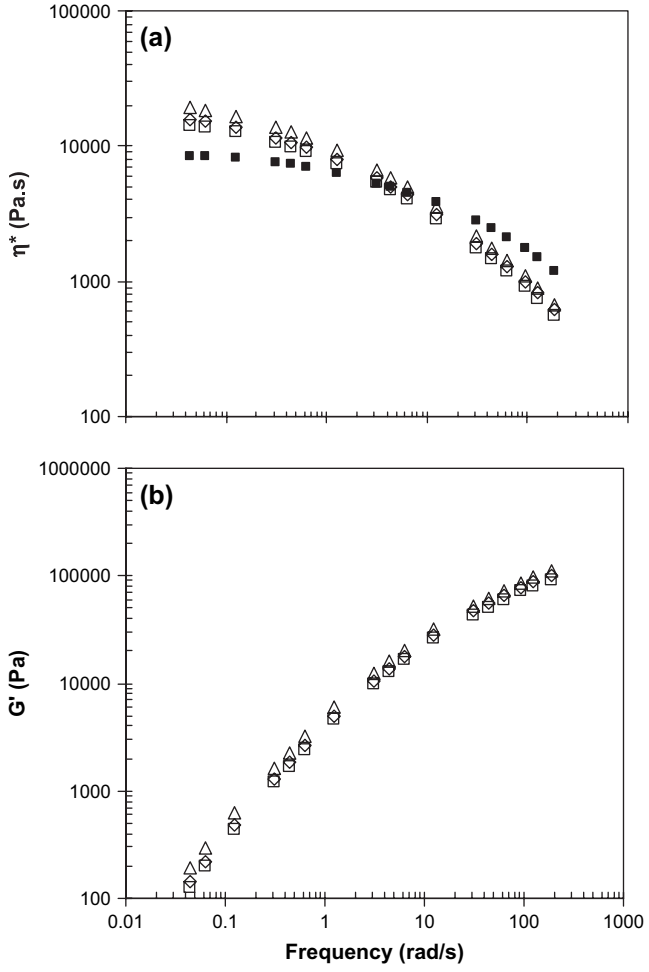

Fig. 2. (a) Complex viscosities; (b) elastic moduli of PP/SiO_2 composites and POE at 200 °C: (□) PP/PP-*g*-MAn 90/10; (△) (PP/PP-*g*-MAn 90/10)−5 wt% SiO_2; (◇) (PP/PP-*g*-MAn 90/10)−5 wt% $mSiO_2$; (■) POE.

of the viscosity of the matrix. Prevention of coalescence of the dispersed phase in the presence of the nanofiller, changes in the interfacial tension [25,26] or stiffening of the interface between the components which slows down the rate of phase separation [27] may be possible explanations, although this issue is still under debate.

3.2.2. Mechanical properties

As shown in Table 2, upon introduction of the elastomer, the elongation at break of the samples increased considerably and they became more ductile, as evidenced by the fact that the values of tensile stress at break were higher than those recorded at yield. At the same time, the modulus and yield stress dropped substantially. The reduction of tensile modulus and yield stress of a rigid PP matrix upon blending with soft elastomer particles is well known and reported in the literature [28,29]. The main purpose of this work is to counteract this effect by selectively reinforcing the PP matrix with rigid filler particles. According to the data in Table 2, improvements in the Young's moduli were seen in all samples upon addition of SiO_2. Additionally all samples retained high values of elongation. The improvements in modulus and yield stress were more pronounced at a component ratio of (PP/PP-*g*-MAn)/POE 80/20 (15% increase in Young's modulus and 4% in yield stress). For this blend ratio, addition of SiO_2 resulted in higher Young's moduli values than the unfilled blend, with a maximum at around 5% SiO_2. Further increasing SiO_2 loading actually resulted in decreased yield stress. Decreases in the tensile properties of composites at high SiO_2 contents have been reported by other researchers [18–20], and may be attributed to the presence of agglomerated nanoparticles, having an increased tendency for breaking and splitting [30]. (PP/PP-*g*-MAn)/POE 80/20 composites containing 5% of $mSiO_2$ had

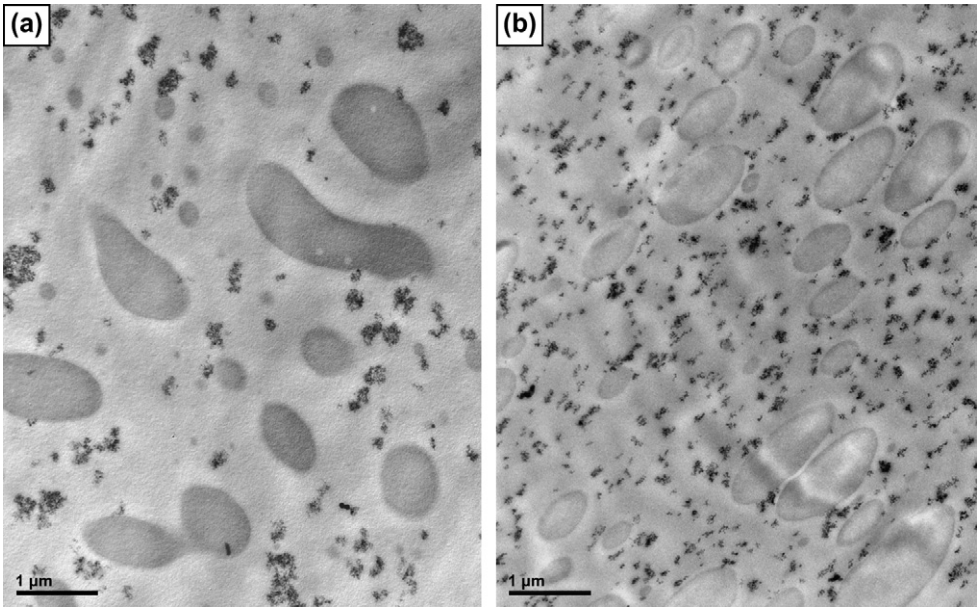

Fig. 3. TEM micrographs of (PP/PP-*g*-MAn)/POE 80/20 TPO composites: (a) 5 wt% SiO_2; (b) 5 wt% $mSiO_2$. Scale bars represent 1 μm.

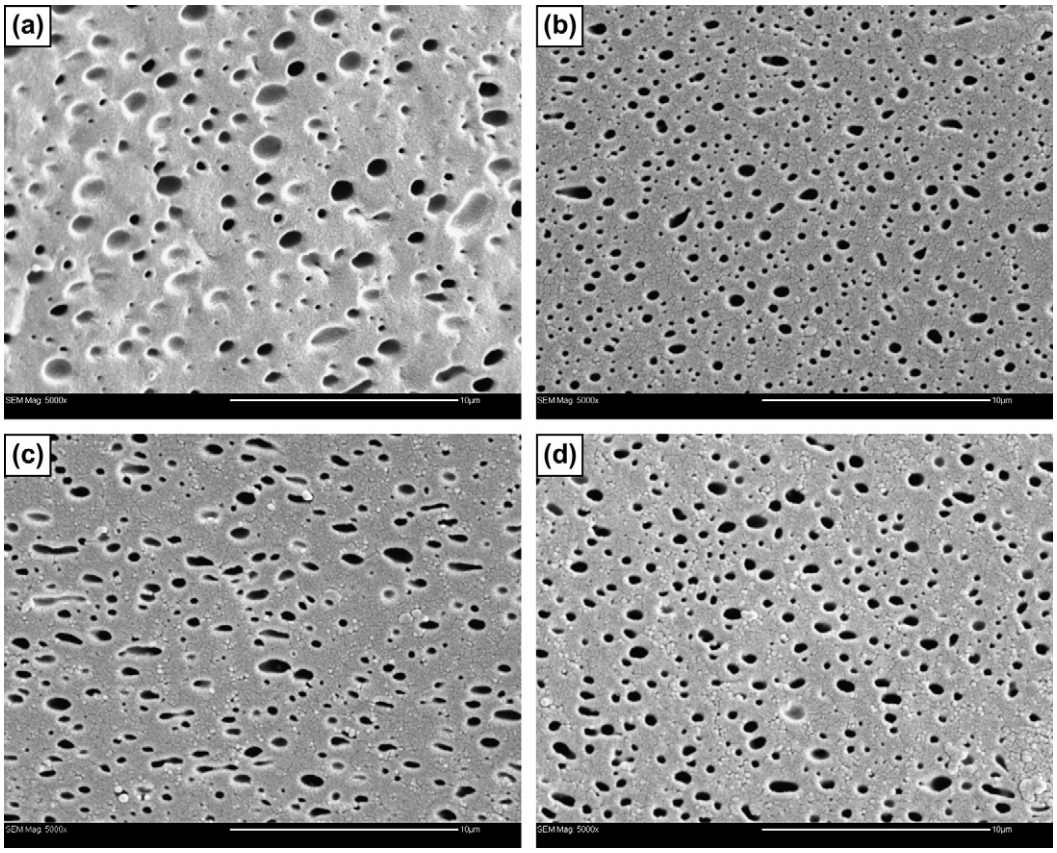

Fig. 4. SEM micrographs of cryotomed and etched surfaces of (PP/PP-*g*-MAn)/POE 80/20 TPO composites; (a) 0 wt% SiO_2, (b) 2 wt% SiO_2, (c) 5 wt% SiO_2, (d) 7 wt% SiO_2. Scale bars represent 10 μm.

slightly better tensile properties than their counterparts containing unmodified SiO_2, apparently because of the improved filler dispersion.

The impact strength of TPO/nanosilica composites based on a matrix containing (PP/PP-*g*-MAn)/POE 80/20 is shown in Fig. 6. As mentioned before the PP-*g*-MAn/PP matrix was very brittle, exhibiting low values of impact strength. Addition of 20 wt% elastomer clearly improved the impact properties of the PP matrix. SEM observations of fractured surfaces of the PP matrix obtained after impact testing, shown in Fig. 7a, revealed relatively smooth surfaces with no matrix yielding, suggesting that the PP matrix experienced a mainly brittle fracture failure mode.

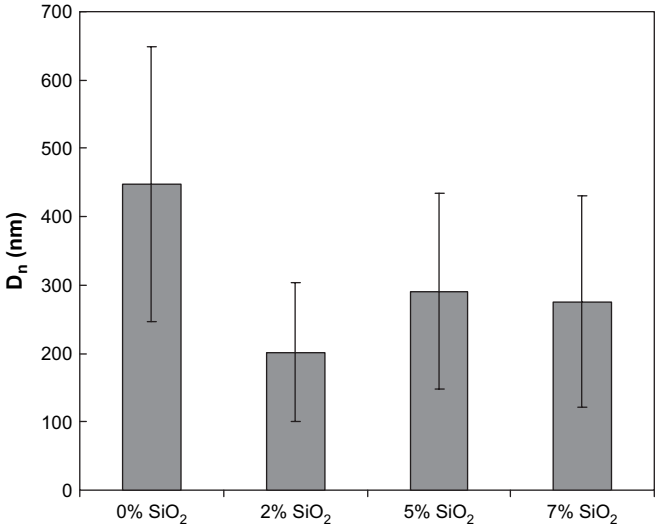

Fig. 5. Number average diameter of POE dispersed phase for (PP/PP-*g*-MAn 90/10)/POE 80/20 composites as a function of SiO_2 content.

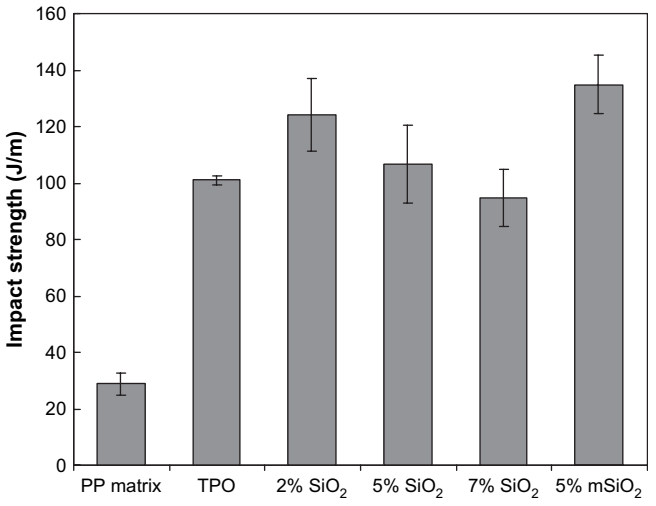

Fig. 6. Notched Izod impact strength of PP/PP-*g*-MAn 90/10 matrix, PP/PP-*g*-MAn 90/10)/POE 80/20 (TPO) and TPO/SiO_2 composites.

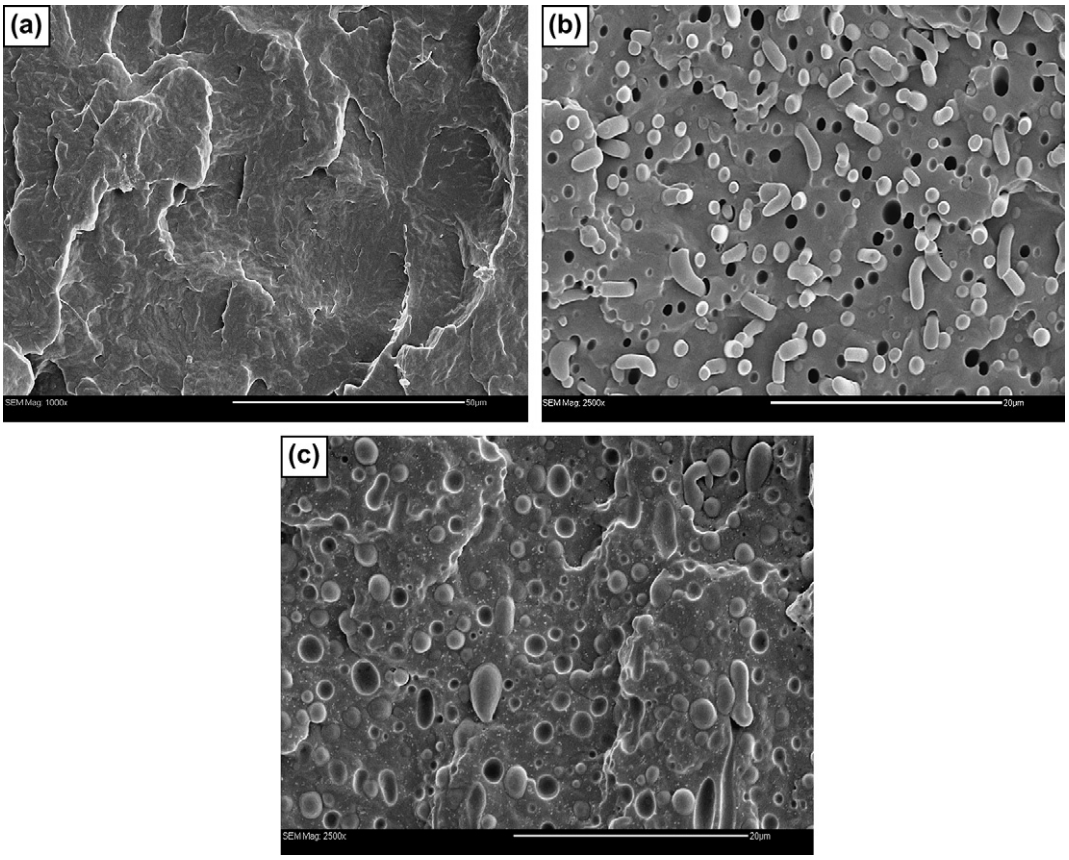

Fig. 7. SEM micrographs of notched Izod impact fracture surfaces of (a) PP/PP-*g*-MAn 90/10; (b) (PP/PP-*g*-MAn)/POE 80/20; (c) (PP/PP-*g*-MAn)/POE 80/20 with 5 wt% $mSiO_2$. The scale bars represent 50 μm in (a), and 20 μm in (b) and (c).

The presence of holes in the TPO blend and the TPO/SiO_2 composites (Fig. 7b and c) suggests that the brittle fracture gave rise to voids due to cavitation of the rubber particles. Cavitation acts to increase impact strength by relieving the volume strain [31]. In addition some deformation of POE particles can be observed, suggesting that toughening also took place through elastic deformation of the dispersed POE particles. Presence of elongated voids is indicative of matrix yielding, corresponding to ductile fracture [32]. According to Chaffin et al. [33] ductile deformation of the dispersed phase can pull along a well-coupled interface, allowing plastic deformation of crystallites, which provides a highly energy-absorbent failure mode. It should be noted that rubber toughening of PP matrices also takes place through a decrease of the spherulite size of PP in the presence of the elastomer [28].

Given that addition of SiO_2 did not alter considerably the impact properties of the matrix PP and did not appear to change the fracture mechanism of the TPO blends, the increase in impact strength of the filled TPOs compared to the unfilled material is possibly due to the reduction in the particle size of the dispersed elastomer phase in the presence of the nanofillers, which acted favourably toward improving toughness [12,34,35].

As evident from Fig. 6, the impact properties of the TPO increased upon addition of only 2 wt% SiO_2. As the filler content increased, whereas the maleated PP content remained the same, there was an increased tendency for filler aggregation, which eventually led to decreased impact strength. Efficient filler dispersion is crucial, as seen by the fact that $mSiO_2$ clearly demonstrated optimum performance. The $mSiO_2$ filled sample showed the most benefits, since its impact strength was the highest at filler loadings of 5 wt%. As mentioned in Figs. 1 and 3, $mSiO_2$ dispersed better than SiO_2 inside the matrix, hence its improved performance.

The flexural properties of the unfilled TPO are compared to those of the composites containing SiO_2 and $mSiO_2$ in Table 3. Both nanosilica filled samples had higher flexural modulus and flexural stress than the unfilled TPO, which provides clear evidence of the reinforcing effect that the filler exerts on the PP matrix. The differences between untreated SiO_2 and surface treated $mSiO_2$ were marginal.

Table 3
Flexural properties of TPO/nanosilica composites

Sample	Flexural modulus (MPa)	Flexural stress[a] (MPa)
TPO	797 ± 24	25.5 ± 0.5
TPO–5 wt% SiO_2	920 ± 39	28.4 ± 1.3
TPO–5 wt% $mSiO_2$	942 ± 64	28.7 ± 1.6

TPO composition (PP/PP-*g*-MAn)/POE 80/20.
[a] Measured at 5% strain.

3.2.3. Thermal properties/crystalline structure

It has been reported previously that the presence of SiO_2 in the PP phase affects its crystallization behaviour [36]. Given that the mechanical properties are largely affected by the crystallinity of the polymers, the effect of SiO_2 on the thermal properties is investigated in this section. Even though the melting points of the PP component in all composites remained constant between 163 and 164 °C, data obtained from the DSC exotherms demonstrate that the addition of SiO_2 into the blends increased the crystallization temperature of PP slightly, suggesting a weak nucleating effect in the matrix (Table 2). The crystallization temperature of $mSiO_2$ filled samples was lower than that of their counterparts containing SiO_2, indicating that surface modification weakens nanosilica's nucleation effect in the PP matrix.

The values of heat of crystallization (Table 2), do not show any particular trend, therefore changes in the total crystallinity of the matrix were probably not responsible for the differences in mechanical properties. Furthermore, XRD studies revealed that the α-type crystal form of PP was predominant, with no evidence of presence of β-phase crystals.

3.2.4. Rheology

Consistently with the results reported on the rheological properties of the PP matrix, the complex viscosities (η^*) and elastic modulus (G') increased only slightly with the addition of nanosilica into the PP/POE blends (Fig. 8). The elastic modulus exhibited a more pronounced increase in the low frequency region, with the largest increase seen at 7 wt% SiO_2. The loss tangent, tan δ, demonstrates clearly that the elasticity of TPO/nanosilica composites increased at filler loadings above 5 wt% and suggests that there is a propensity for filler aggregation and possibly interactions between nanosilica aggregates above this loading. Addition of $mSiO_2$ had virtually no effect on the rheology of the matrix.

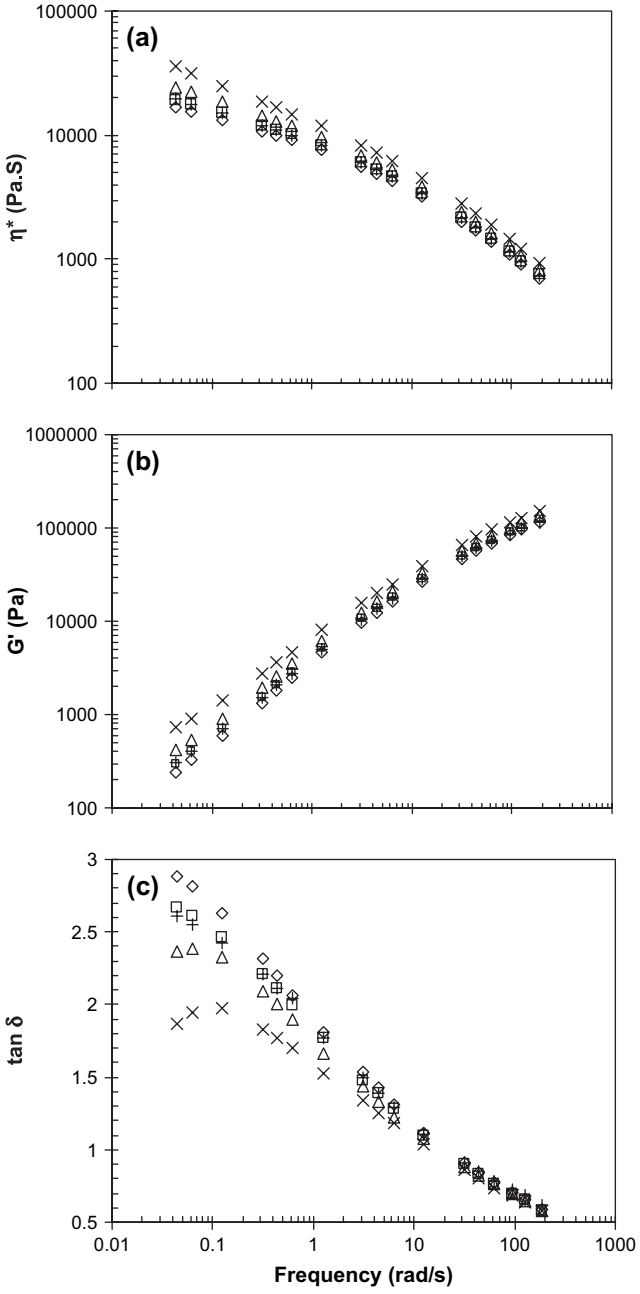

Fig. 8. (a) Complex viscosity (η^*), (b) elastic modulus (G'), and (c) tan δ of (PP/PP-*g*-MAn 90/10)/POE 80/20 composites as a function of frequency at 200 °C; (◇) 0%, (□) 2% SiO_2, (△) 5% SiO_2, (×) 7% SiO_2, (+) 5% $mSiO_2$.

4. Conclusions

Addition of PP-*g*-MAn into PP was necessary to reduce large SiO_2 aggregates and achieve good dispersion of the filler within the polymer matrix. The surface treated $mSiO_2$ dispersed more efficiently in a PP-*g*-MAn/PP matrix than untreated SiO_2.

When added into a TPO blend nanosilica localized exclusively in the PP/PP-*g*-MAn matrix phase and formed a separated microstructure that is desirable for optimum reinforcement. The size of the dispersed POE phase decreased upon incorporation of nanosilica.

Tensile moduli, impact and flexural properties of TPO/nanosilica composites showed improvements at low loadings of nanosilica, indicating a good balance of stiffness and toughness. Given that the crystallinity of the polymer matrix remained unaffected, these improvements were attributed to the reinforcement effect of the filler, as well as the reduction in the particle size of the dispersed elastomer phase. A weak nucleation effect in the PP phase, represented by an increase in the crystallization temperatures of the composites, was noted in the presence of SiO_2 particles.

Acknowledgements

Financial support was provided by the Ontario Centres of Excellence (OCE)/Emerging Materials Knowledge (EMK) program of the Centre for Materials and Manufacturing and by a scholarship from the Chinese Scholarship Council. The authors wish to thank Nanocor Inc. and Degussa Corp. for providing clay and silica samples, respectively, and ExxonMobil

and E.I. DuPont Canada for supplying the polymers used in this work.

References

[1] Karger-Kocsis J, Kallo A, Kuleznev VN. Polymer 1984;25(2):279–86.
[2] Van Der Wal A, Mulder JJ, Oderkerk J, Gaymans RJ. Polymer 1998; 39(26):6781–7.
[3] Yu TC. Polym Eng Sci 2001;41(4):656–71.
[4] McNally T, McShane P, Nally GM, Murphy WR, Cook M, Miller A. Polymer 2002;43(13):3785–93.
[5] Choudhary V, Varma HS, Varma IK. Polymer 1991;32(14):2534–40.
[6] Long Y, Shanks RA. J Appl Polym Sci 1996;61(11):1877–85.
[7] Jancar J, Dibenedetto AT. J Mater Sci 1995;30(6):1601–8.
[8] Premphet K, Horanont P. J Appl Polym Sci 2000;76(13):1929–39.
[9] Su X, Hua Y, Qiao J, Liu Y, Zhang X, Gao J, et al. Macromol Mater Eng 2004;289(3):275–80.
[10] Uotila R, Hippi U, Paavola S, Seppala J. Polymer 2005;46(19): 7923–30.
[11] Long Y, Shanks RA. J Appl Polym Sci 1996;62(4):639–46.
[12] Lee H, Fasulo PD, Rodgers WR, Paul DR. Polymer 2005;46(25):11673–89.
[13] Lim JW, Hassan A, Rahmat AR, Wahit MU. J Appl Polym Sci 2006; 99(6):3441–50.
[14] Lee KY, Goettler LA. Polym Eng Sci 2004;44(6):1103–11.
[15] Maiti M, Bandyopadhyay A, Bhowmick AK. J Appl Polym Sci 2006; 99(4):1645–56.
[16] Mehta S, Mirabella FM, Rufener K, Bafna A. J Appl Polym Sci 2004; 92(2):928–36.
[17] Mishra JK, Hwang KJ, Ha CS. Polymer 2005;46(6):1995–2002.
[18] Rong M, Zhang M, Zheng Y, Zeng H, Walter R, Friedrich K. Polymer 2001;42(1):167–83.
[19] Wu C, Zhang M, Rong M, Friedrich K. Comp Sci Technol 2002; 62(10–11):1327–40.
[20] Bikiaris DN, Vassiliou A, Pavlidou E, Karayannidis GP. Eur Polym J 2005;41(9):1965–78.
[21] Bikiaris DN, Papageorgiou GZ, Pavlidou E, Vouroutzis N, Palatzoglou P, Karayannidis GP. J Appl Polym Sci 2006;100(4):2684–96.
[22] Austin JR, Kontopoulou M. Polym Eng Sci, in press.
[23] Kontopoulou M, Austin JR, Liu Y, Parent JS. In: Proceedings PPS-2005, Quebec City; 2005.
[24] Khan SA, Prud'homme RK. Rev Chem Eng 1987;4(3–4):205–70.
[25] Khatua BB, Lee DJ, Kim HY, Kim JK. Macromolecules 2004;37(7): 2454–9.
[26] Ray SS, Pouliot S, Bousmina M, Utracki LA. Polymer 2004;45(25): 8403–13.
[27] Zhang Q, Yang H, Fu Q. Polymer 2004;45(6):1913–22.
[28] Copolla F, Greco R, Martucelli E, Kammer HW, Kummerlowe C. Polymer 1987;28(1):47–56.
[29] van der Wal A, Nijhof R, Gaymans RJ. Polymer 1999;40(22): 6031–44.
[30] Li JX, Silverstein M, Hiltner A, Baer E. J Appl Polym Sci 1994;52(2): 255–67.
[31] Borggreve RJM, Gaymans RJ, Eichenwald HM. Polymer 1989;30(1): 78–83.
[32] van der Wal A, Gaymans RJ. Polymer 1999;40(22):6067–75.
[33] Chaffin KA, Bates FS, Brant P, Brown GM. J Polym Sci Part B Polym Phys 2000;38:108–21.
[34] Wu S. J Appl Polym Sci 1988;35(2):549–61.
[35] Wu S. Polymer 1985;26(12):1855–63.
[36] Qian J, He P, Nie K. J Appl Polym Sci 2004;91(2):1013–9.